Analyst

Accepted Manuscript

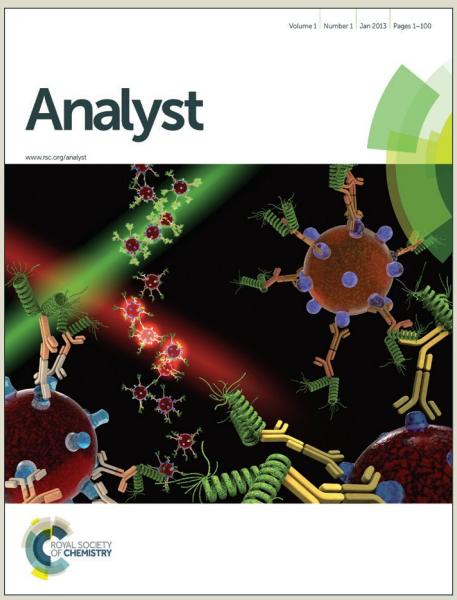

ROYAL SOCIETY OF CHEMISTRY

www.rsc.org/analyst

Journal Name

ARTICLE

Specific interactions of leucine with disaccharides by electrospray ionization mass spectrometry: Application for rapid differentiation of disaccharide isomers in combination with statistical analysis

Received 00th January 20xx,
Accepted 00th January 20xx

DOI: 10.1039/x0xx00000x

www.rsc.org/

Hang Yuan[a], Jianxi Ying[a], Peiran Deng[a],Peng Chen[a],Jinwen Shi[b], Yan Liu[a*], Xiang Gao[b*], Yufen Zhao[a,c]

The identification of carbohydrate isomers, including mono units, linkage positions and anomeric configurations, remains an arduous subject. In this study, the natural amino acid–leucine (Leu) was found to specifically interact with cellobiose (Cello) to form a series of potassium adducts as $[Cello+Leu+K]^+$, $[Cello+2Leu+K]^+$, and $[2Cello+Leu+K]^+$ in gas phase using mass spectrometry. By using CID-MS/MS, these complexes produced specific fragmentation patterns from the sugar backbone cleavage instead of non-covalent interactions. Moreover, their fragment distributions were dependent on the ratios of Cello-to-Leu in complexes and the fragmentation pathways of potassium-cationized disaccharides (Dis) were remarkably changed with leucine binding. It should be pointed that the ternary complex $[2Cello+AA+K]^+$ was unique for leucine among all the twenty natural amino acids. The $[2Dis+Leu+K]^+$ complex produced the most informative fragments by tandem mass spectrometry, which was successfully applied for rapid and efficient discrimination of twelve glucose-containing disaccharide isomers in combination with statistical analysis including PCA and OPLS-DA. The methodology developed here not only provides a novel analytical approach for the differentiation of disaccharide isomers, but also brings a new sight towards the interactions of amino acids with disaccharides.

1. Introduction

Carbohydrates are not only regarded as a major energy source and structure components, but are also involved in multiple forms of biological processes.[1-3] Proteins including specific enzymes, anti-carbohydrate antibodies and lectins, which interact with carbohydrates non-covalently, occur ubiquitously in cell differentiation, immune response and cell recognition.[4-7] In recent years, many approaches have been developed to study the processes of saccharides-based molecular recognition. For example, synthetic lectins, chemical responsive dyes, and fluorescent sensors were designed as glycan receptors.[8-11] However, these procedures were still constrained by the complex structures of proteins and oligosaccharides and the challenge of carbohydrate receptor designation. Hence, determinations of the non-covalent interactions of amino acids and disaccharides as the smallest oligosaccharides are essential prerequisite for elucidating the underlying principle of protein-carbohydrate interactions.

[a] Department of Chemical Biology, College of Chemistry and Chemical Engineering, Key Laboratory for Chemical Biology of Fujian Province, Xiamen University, Xiamen, Fujian, China, 361005. E-Mail：stacyliu@xmu.edu.cn
[b] School ofPharmaceutical Sciences, Xiamen University,Xiamen,Fujian,China, 361102.E-Mail: xgao@xmu.edu.cn
[c] Key Laboratory of Bioorganic Phosphorus Chemistry and Chemical Biology (Ministry of Education), Department of Chemistry, Tsinghua University, Beijing, China, 100084.

Currently, nuclear magnetic resonance (NMR)[12-15] and liquid chromatography (HPLC) [16-19] have been utilized to character the interactions of oligosaccharides and other molecules. Specifically, mass spectrometry (MS) could offer a fast, accurate and sensitive methodology to investigate non-covalent complexes for the structural identification of saccharides and the discrimination among isomeric disaccharides which were different in monosaccharide composition, glycosidic linkage, and anomeric configurations.[20] Recently, many approaches have been developed for the rapid discrimination of carbohydrate isomers based on their intrinsic features, such as ion/molecular reactions,[21] migration rates in ion mobility mass spectrometry,[22] the infrared multiple photon dissociation at different wavelength[23,24] and so on. Especially, collision induced dissociation (CID) is the most common and well-established approach for the elucidation of oligosaccharides. For example, modified/unmodified amino acids coordinated with transition metal ions have been used for identification and quantification of monosaccharides by CID-MS/MS.[25-27] The differentiation of isomeric hexose disaccharides have been accomplished by calculating the relative abundance ratios of product ions generated from glycosidic bond cleavage.[28,29] Additionally, the CID-MS/MS analysis of the deprotonated disaccharide dimers and anion adducts have also been applied to distinguish disaccharides according to the characteristic product ions with different intensities in negative ion mode.[30-32] However, it is laborious to discriminate abundant disaccharide isomers by comparison of the intensity ratios of product ions.

In our previous work, the natural amino acid L-valine could specifically interact with hexose to form complex ion $[2Val+Hex+K]^+$, which has been successfully used to discriminate monosaccharide isomers through the dissociation of hexose covalent bonds by ESI-MS/MS.[33] Herein, we systematically investigated the interactions of 20 natural amino acids (AAs) and cations (H^+, NH_4^+, Li^+, Na^+, and K^+) with disaccharides (Dis) such as cellobiose (Cello) in positive ion mode by using ESI-MS equipped with two different mass analyzers including ion trap (IT) and quadrupole time-of-flight (Q-TOF) respectively. It is demonstrated that Cello-AAs complexes such as $[Cello+2Leu+K]^+$ and $[2Cello+Leu+K]^+$ are readily formed with high relative abundances. Importantly, the binding of leucine could induce the conformational changes of disaccharide complexes and subsequently lead to cross-ring cleavage of sugar backbones. Then, the formation of the unique complex $[2Cello+Leu+K]^+$ as well as its fragmentation pathways were proposed and confirmed by ^{18}O-labeling experiment and ^1H NMR analysis. The above complex model is also appropriate for all twelve glucose-containing disaccharides with different linkages, mono units, and anomeric configurations and their fragmentation patterns are closely associated with their chemical structures. Based on the characteristic fragments, twelve disaccharide isomers could be unambiguously discriminated by statistical analysis including PCA and OPLS-DA. The specific interactions of leucine with disaccharides by ESI-MS in combination with statistical analysis offer a convenient approach for disaccharide isomers differentiation.

2. Experimental

2.1. Materials and Reagents

Twelve glucose-containing disaccharide isomers, namely kojibiose, sophorose, nigerose, laminaribose, maltose, cellobiose, isomaltose, gentiobiose, sucrose, turanose, maltulose, and palatinose, were purchased from J&K Chemical Ltd. (Beijing, China) with the purity of 99%. Twenty common amino acids, inorganic salts (LiCl, NaCl, KCl, NH_4Cl) and $H_2{}^{18}O$ were obtained from Sigma-Aldrich (St. Louis, MO, USA). All reagents were used without further purification. HPLC-grade methanol was purchased from Tedia (Fairfield, OH, USA). Distilled water was prepared by Milli-Q water purification system (Millipore, Bedford, MA). All disaccharide solutions were freshly prepared by dissolving the corresponding disaccharides (0.1 mM), amino acids (0.1 mM), and inorganic salts (10 μM) in the solvent of water/methanol (1/1, v/v) before the experiments. Cellobiose with one ^{18}O atom labeling at anomeric hydroxyl group was prepared by a method of literature.[34] In brief, 0.5 mg cellobiose was dissolved in 300 μL $H_2{}^{18}O$ in 1.5 mL polypropylene microcentrifuge tube. Then, the above mixture was incubated in water bath at 60℃ for about 24 hours. The labeling process was monitored by using mass spectrometry.

2.3. Mass Spectrometry Analysis

Mass spectra were acquired on two instruments equipped with electrospray ionization source and different analyzers, containing ion-trap (Amazon SL, Bruker Daltonics, Germany) and Q-TOF (Bruker Daltonics, Germany). The ESI-MS conditions were as follows: (1) ESI ion-

trap mass spectrometer (ESI-IT-MS): Spray voltage -4.0 kV, nebulizer gas 8.0 psi, dry gas 4.5 L/min, dry temperature 300℃. The collision energy for the CID was approximately 0.25~0.32 V. The precursor ion was isolated in the width of 2.0 *m/z*. Each spectrum was the average of 15 scans. (2) ESI-Q-TOF MS: Spray voltage -4.0 kV, nebulizer gas 6.0 psi, dry gas 2.0 L/min, and dry temperature 300℃. The collision energy was ranged from 6 eV to 12eV.

In both instruments above, the injection rate was set at 180 μL/h. The mass scan range was generally from *m/z* 100 to 1200. Each sample was analyzed at least six times on different day. The resultant product ions with relative peak intensity higher than 5% were selected for the construction of statistical model.

2.4. ^{1}H NMR Analysis

The ^{1}H NMR measurement was performed on Bruker 500 MHz NMR spectrometer at ambient temperature. Cellobiose (0.1 mmol) was incubated with leucine (0.1 mmol) and KCl (0.01mmol) in 500 μL D_2O. The above reaction was tracked by ^{1}H NMR at different reaction time. The ^{1}H chemical shift was calibrated by the TMS (δ=0.0 ppm) in D_2O.

2.5. Statistical Analysis

Fragments together with their relative abundance (>5%) generated from the tandem mass spectrometry of the $[2Dis+Leu+K]^+$ (*m/z* 854) were introduced to SIMCA-P+ version 12.0 (Umetrics, Sweden) for principle component analysis (PCA) and orthogonal partial least squares discriminant analysis (OPLS-DA).[35,36] The results were exhibited in the form of score plots, where each point denoted an independent sample's analysis. Both of them were accomplished with unit variance scaling and qualified by the cross-validation parameters Q^2 and R^2X which indicated the predictability and total variables explanation respectively. No standards of classification success were provided, but R^2 and Q^2 values more than 0.5 in all the statistical models belonged to the appropriate models.[37]

3. Results and discussion

Leucine could interact with disaccharides to form ternary complexes in gas phase

The structural formulas of twelve isomeric glucose-containing disaccharides investigated in this work were presently described in Table 1. Firstly, the solution of cellobiose (Glcβ1-4Glc) with leucine and potassium ion was inspected by ESI-IT-MS in positive ion mode. A series of leucine adduct ions, such as $[Cello+Leu+H]^+$ at *m/z* 474, $[Cello+Leu+K]^+$ at *m/z* 512, $[Cello+2Leu+K]^+$ at *m/z* 643, and $[2Cello+Leu+K]^+$ at *m/z* 854, were detected (Fig. 1). Furthermore, the non-covalent interactions of cellobiose with twenty natural amino acids (AAs) were systematically examined using ESI-IT-MS and ESI-Q-TOF-MS. The results exhibited in Table S1 showed that ternary adducted ions $[Cello+2AA+K]^+$ were observed for valine (Val), isoleucine (Ile), leucine (Leu), and serine (Ser) by using ESI-IT-MS. No adducted ions were detected for other sixteen amino acids suggesting that the amino acids with acidic, basic, or aromatic side chains were assumed to hinder the formation of ternary adducts. Whereas, amino acids with aliphatic or hydrophobic functional groups, such as Val, Ile, and Leu (except for Ser), were beneficial to obtain the ternary adduct ions $[Cello+2AA+K]^+$. Interestingly, the ternary adduct ion $[2Cello+AA+K]^+$could be detected only for leucine by using both mass spectrometers, indicating that the specific hydrophobic side chain of leucine and the intrinsic size of metal ion exerted the remarkable effects on the formation of Cello/AAs/potassium ternary adducts.

Table 1 List of glucose-containing disaccharides

composition	Name	Linkage Type
Glc-Glc	Kojibiose	Glcα1-2Glc
	Sophorose	Glcβ1-2Glc
	Nigerose	Glcα1-3Glc
	Laminaribiose	Glcβ1-3Glc
	Maltose	Glcα1-4Glc
	Cellobiose	Glcβ1-4Glc

	Isomaltose	Glcα1-6Glc
	Gentiobiose	Glcβ1-6Glc
Glc-Fru	Sucrose	Glcα1-2Fru
	Turanose	Glcα1-3Fru
	Maltulose	Glcα1-4Fru
	Palatinose	Glcα1-6Fru

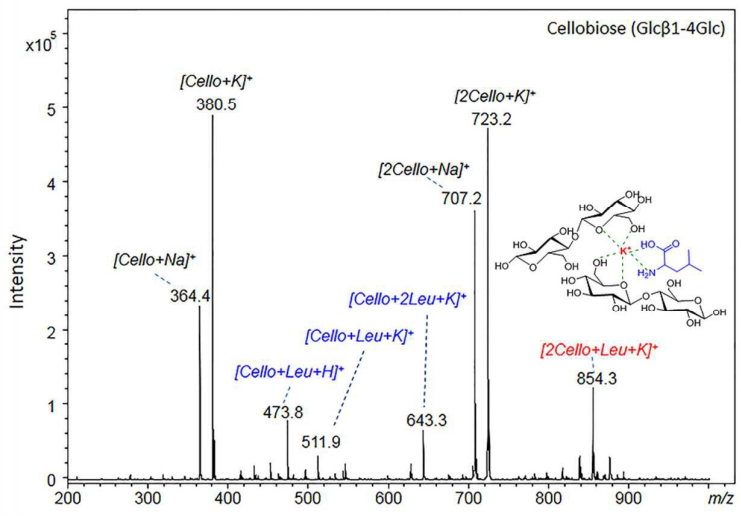

Fig.1 Interactions of cellobiose (Glcβ1-4Glc) with leucine by ESI-IT-MS in positive ion mode.

In order to study the influences of the cation on the chemical structures of gas-phase Cello/Leu adducts, tandem mass spectrometry analysis was performed and presented in Fig. 2. It was found that no adducts for NH_4^+ was observed, simultaneously, the dissociation patterns of ternary complexes were mainly determined by the binding cations (H^+, Li^+, Na^+, and K^+) and the ratios of Cello to Leu in potassium adducts. As shown in Fig. 2A-C, the dominant dissociation pathways of Cello/Leu complexes were the loss of a cellobiose from H^+ adduct or a leucine from Li^+ and Na^+ adducts respectively. Apparently, leucine could effectively inhibit the sugar skeleton cleavage in relative to the cationized (H^+, Li^+, and Na^+) disaccharides complexes.[28, 29] Whereas, the fragmentation patterns of the potassium adducts were discovered to be scaled with the Cello/Leu ratios within the ternary complexes. As shown in Fig. 2D and 2E, the product ions of *m/z* 452 and *m/z* 392 corresponding to $[Cello+Leu+K-C_2H_4O_2]^+$ and $[Cello+Leu+K-2C_2H_4O_2]^+$ were generated with different relative abundances from the cross-ring cleavage of both complexes $[Cello+Leu+K]^+$ and $[Cello+2Leu+K]^+$. For the fragmentation of $[2Cello+Leu+K]^+$ at *m/z* 854, several dominant product ions including *m/z* 723, *m/z* 663, *m/z* 603, *m/z* 543, and *m/z* 483 were observed in the ESI-IT-MS/MS spectrum (Fig. 2F). Three types of dissociation pathways were involved: (1) the neutral loss of a molecule of leucine (-131Da) for ion at *m/z* 723; (2) cross-ring cleavage ions at *m/z* 663, *m/z* 603, *m/z* 483, and *m/z* 393; (3) glycosidic bond cleavage ion at *m/z* 543 (*m/z* 723→*m/z* 543) with the neutral loss of a monosaccharide (-180Da). The fragment patterns mainly arose from the skeleton cleavage of sugar-ring in the ternary complex other than the simple dissociation of non-covalent interactions for the potassium-cationized disaccharides. It means that leucine could effectively revise the fragmentation pathways of disaccharide potassium adducts in which was difficult to obtain fragment ions generating from cross-ring cleavage.[38] As previous research reported that the precursor ions were more sensitive to dissociate along the fragile bond under CID-MS/MS condition,[39] it was reasonable to deduce that non-covalent interaction of potassium adducted disaccharides dimer was greatly increased in comparison of the covalent bond of sugar-ring by the attachment of leucine. Although the basic mechanism of sugar-ring cleavages induced by leucine binding could not be completely uncovered by the present study, it is speculated that leucine might stabilize the gas phase conformation of potassium-disaccharides adducts and make the non-covalent interactions stronger than the covalent sugar skeleton.

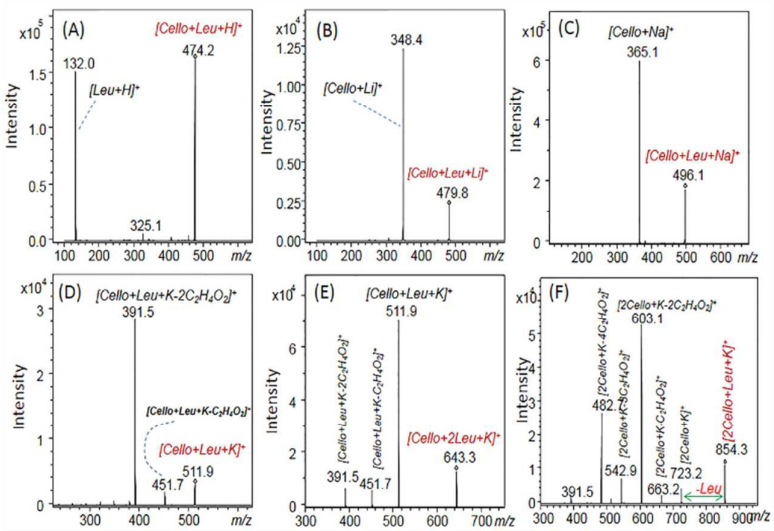

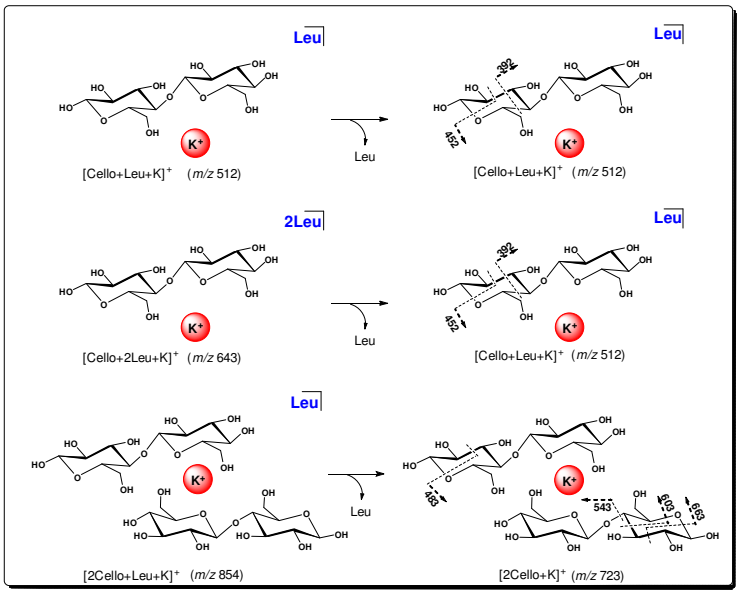

Fig. 2 ESI-IT-MS/MS spectra of Cello/Leu complexes coordinated with different cations in positive ion mode. (A) $[Cello+Leu+H]^+$ at *m/z* 474; (B) $[Cello+Leu+Li]^+$ at *m/z* 480; (C) $[Cello+Leu+Na]^+$ at *m/z* 496; (D) $[Cello+Leu+K]^+$ at *m/z* 512; (E) $[Cello+2Leu+K]^+$ at *m/z* 643; (F) $[2Cello+Leu+K]^+$ at *m/z* 854. The proposed sugar-skeleton fragmentation pathway of potassium adducts were displayed on the bottom.

Since the cross-ring cleavages were informative for structural characterization of disaccharides, [40, 41] ESI-MS/MS spectrum of $[2Cello+Leu+K]^+$ at *m/z* 854 with the most abundant cross-ring cleavage ions was chosen for further discussion. As described earlier, the first step of its dissociation was the elimination of a leucine (-131 Da) to form $[2Cello+K]^+$ion at *m/z* 723. Herein, stable isotope ^{18}Olabeling experiments were applied to confirm the leucine elimination and cross-ring cleavage. With the anomeric hydroxyl oxygen of cellobiose labeled by ^{18}O atom, the ternary cluster of $[2Cello\ (^{18}O_2)+Leu+K]^+$ at *m/z* 858 was detected with 4 Da mass shift by ESI-IT-MS. In the CID-MS/MS spectrum of $[2Cello\ (^{18}O_2)+Leu+K]^+$ at *m/z* 858, the fragment peak at *m/z* 727 ($[2Cello\ (^{18}O_2)+K]^+$) with two ^{18}O atoms verified the neutral loss of leucine (-131Da) (Fig. 3A). The fragment ion *m/z* 665 corresponding to the neutral loss of $C_2H_4{}^{16}O^{18}O$ (-62Da) of the precursor ion *m/z* 727 proposed that the cross-ring cleavage primarily occurred from the reducing end, and continued sequentially along the sugar skeleton, i.e. the loss of $C_2H_4O_2$ (-60Da) to produce the ion of *m/z* 605, the glycosidic bond cleavage to obtain ion at *m/z* 545. Then,

another ^{18}O-labeling carbonyl position at the reducing end was lost to generate the ion at *m/z* 483. In view of the interaction of potassium-crown ether in gas phase, [42] the possible interaction mechanism and dissociation pathways of the ternary cluster were elucidated in Scheme 1.

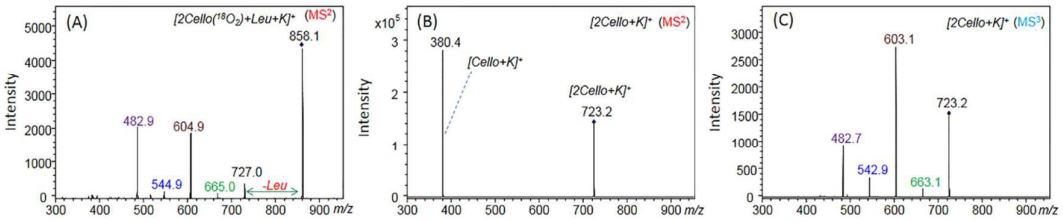

Fig. 3 Analysis of ternary Cello/Leu/potassium complex by ESI tandem mass spectrometry in positive ion mode. (A)ESI-IT-MS/MS of ^{18}O labeled complex [2Cello($^{18}O_2$)+Leu+K]$^+$ at *m/z* 858 with two ^{18}O atoms; (B) ESI-IT-MS/MS of [2Cello+K]$^+$ at *m/z* 723 isolated from the full-scan MS in Fig. 1; (C)ESI-IT-MS^3 of product ion [2Cello+K]$^+$ at *m/z*723 generated from parent ion at *m/z* 854.

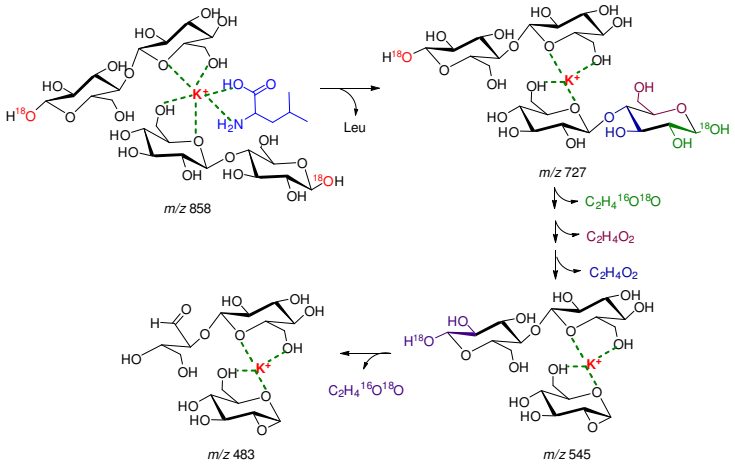

Scheme 1 The possible fragmentation pathways for [2Cello ($^{18}O_2$)+Leu+K]$^+$complex.

Interestingly, the parent ion [2Cello+K]$^+$ at *m/z* 723 isolated directly from full-scan MS (Fig. 1) produced a predominant fragment ion at *m/z* 381 by a neutral loss of cellobiose in tandem mass spectrometry (Fig. 3B). However, more fragments including *m/z* 663, *m/z* 603, *m/z* 543, and *m/z* 483 derived from the cross-ring cleavage of the product ion at *m/z* 723 were observed, where *m/z* 723 was from the leucine loss of the parent ion [2Cello+Leu+K]$^+$at *m/z* 854 (Fig. 3C).These dissimilar fragment pathways were distinctly caused by the involvement of leucine, indicating that the conformation changes induced by leucine binding still played leading roles on fragmentations in gas phase even though leucine has been eliminated from the parent ion of [2Cello+Leu+K]$^+$. This furnished another evidence that leucine could strengthen the non-covalent interactions of potassium-cationized disaccharides and thereby regulate their gas phase conformation, leading to the reducing ring opening other than non-covalent dissociations.

To certify the amino acids/disaccharides complexes did not covalently form in solution phase, ^{1}HNMR was utilized to track the mixture of cellobiose, leucine and potassium salt in aqueous phase incubating at room temperature in 2 hours (Fig. S1). As expected, no new peaks were observed during the incubation process by comparison to the ^{1}H NMR spectra of standard cellobiose and leucine as background, suggesting that there was no occurrence of chemical reactions between cellobiose and leucine in working solution.

The application of the ternary complex [2Dis+Leu+K]$^+$ for rapid discrimination of disaccharide isomers

As a further test of the stabilizing effect of leucine on the conformations of disaccharides/potassium adducts, the ternary cluster of $[2Dis+Leu+K]^+$ was introduced to other eleven glucose-containing disaccharides using ion-trap (Table 2) and Q-TOF (Table S2) mass spectrometers, respectively. It is worthy to note that the general dissociation pathways in CID-MS/MS spectra are the neutral loss of leucine together with the glycosidic bonds dissociation and cross-ring cleavages.

Table 2 ESI-IT-MS/MS analysis of the ternary $[2Dis+Leu+K]^+$complex at *m/z* 854.

Structure	Relative abundance of fragment ions (%, data was exhibited as means S.E.M.)													
	836	723	663	633	603	561	543	512	501	483	453	441	393	381
Glcα1-2Glc					13±1		5±0			100±0				
Glcβ1-2Glc		5±1			16±0		16±0			100±0			6±1	
Glcα1-3Glc		100±0		84±1	5±0	57±2	30±1	11±1	48±1		97±3	48±0		31±2
Glcβ1-3Glc		38±1		5±0	11±1	8±1		27±1	10±1		100±0	19±0		25±0
Glcα1-4Glc		100±0			19±1	9±1			10±0	7±0		25±0		
Glcβ1-4Glc		7±0			100±0		14±0			49±1				
Glcα1-6Glc	10±1	22±1	60±1		100±0		43±1			39±1				
Glcβ1-6Glc		46±1	49±1		100±0		12±0			6±0				
Glcα1-2Fru		100±0				6±0		5±0	9±1			11±0		
Glcα1-3Fru		57±3		100±0		59±2	54±2		46±3		58±5	32±1		10±1
Glcα1-4Fru		100±0			22±1	10±0			11±1		7±1	25±1		
Glcα1-6Fru		100±0		61±1		9±0	5±0		6±0	6±0				

In addition, the fragmentation ions and their relative abundances are closely related to the structure of disaccharides including mono units, linkage positions and anomeric configuration under the same experimental conditions. For example, as shown in Fig. 4A, the ternary complex ion of maltose (Glcα1-4Glc) produced several characteristic fragment ions including *m/z* 633, *m/z* 561, *m/z* 501, and *m/z* 441 as compared with cellobiose (Glcβ1-4Glc) (Fig. 2F). For β isomers of Glc-Glc, linkage positions showed a significant influence on the formations of base peaks, such as the ion at *m/z* 483 for 1,2-linkage, *m/z* 453 for 1,3-linkage, and *m/z* 663 for 1,6-linkage (Fig.4B-D). As a general trend, the decomposition behaviors for α isomers of Glc-Glc and Glc-Fru were also varied by linkage positions (Fig. S2 and S3). Rationally, the fragmentation of the ternary complex $[2Dis+Leu+K]^+$ could be used as the basis for isomers discrimination. Although there are many characteristic product ions formed with different intensities and ratios for each disaccharide, it is laborious and time-consuming to compare the specific tandem mass spectrum with others for disaccharide isomers differentiation among abundant isomers.

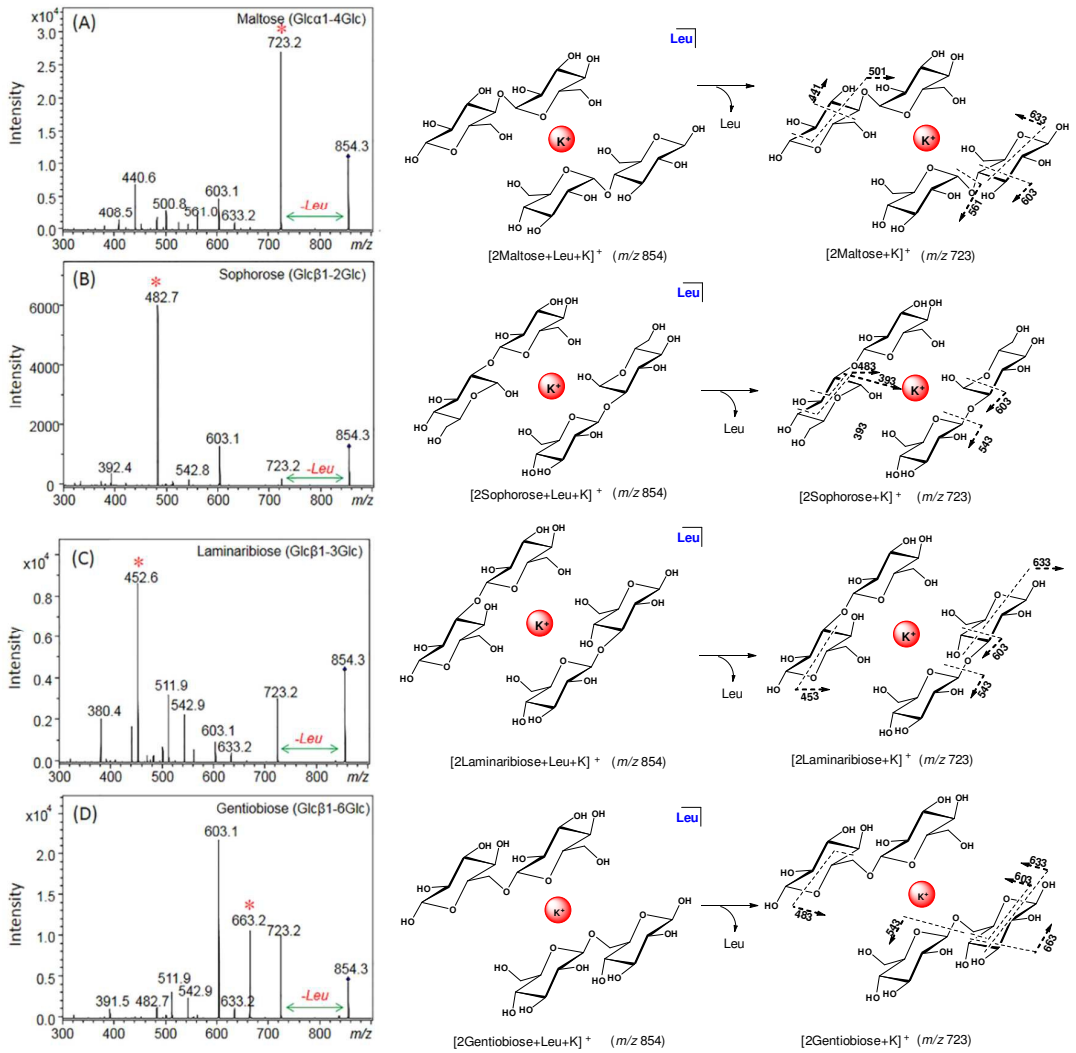

Fig.4 ESI-IT-MS/MS spectra of $[2Dis+Leu+K]^+$ of four glucopyranosyl-glucose disaccharides in positive ion mode. (A) Maltose (Glcα1-4Glc); (B) Sophorose (Glcβ1-2Glc); (C) Laminaribiose (Glcβ1-3Glc); (D) Gentiobiose (Glcβ1-6Glc). The characteristic fragment ions for disaccharides were marked by "*". The proposed sugar-skeleton fragmentation pathways of potassium adducts were displayed on the right.

Multivariate analysis, especially for PCA and OPLS-DA, has been widely used for the statistical analysis of complex data sets. These techniques could be accessed to provide low-dimensional representations of complex datasets through visually interpretable scores plots.[43-46] In this work, the unsupervised multivariate data analysis, PCA, was firstly used to determine whether the fragments of $[2Dis+Leu+K]^+$ were sufficient to distinguish isomeric disaccharides. As illustrated in Fig. 5A, the first two components derived from the data of IT-MS/MS accounted approximately for 60% of the variation. Each color was corresponded to one of the twelve disaccharides, which clearly revealed that the independent cluster was obtained for each different disaccharide. Similarly, the first two PCs (PC1 and PC2) explained about 64% of the original data sets of Q-TOF-MS/MS with turanose as outlier (Fig. 5B). Additionally, the intragroup clusters in the PCA model of IT-MS/MS were tighter than that of Q-TOF-MS/MS, indicating that better reproducibility could be obtained by ESI-IT-MS.

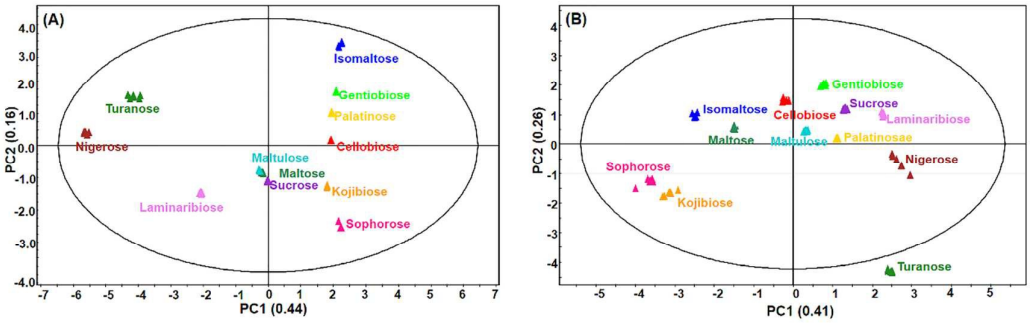

Fig.5 PCA score plots of $[2Dis+Leu+K]^+$ complexes of twelve glucose-containing disaccharides using ESI-IT-MS/MS (A) and ESI-Q-TOF-MS/MS (B) respectively. Each disaccharide complex was determined for six times.

The PCA models afforded a summary of twelve disaccharides through clustering each disaccharide, which mainly emphasized on the interclass diversities of product ions. Meanwhile, OPLS-DA models as the supervised method was further performed in order to enhance intergroup differences based on characteristic ions with different relative intensities. As shown in Fig. 6 and Fig. S4, all twelve disaccharides could be successfully recognized and grouped in terms of mono units, linkage positions, and anomeric configurations based on the IT-MS/MS or Q-TOF-MS/MS data sets. For example, four kinds of linkage positions could be excellently classified by OPLS-DA with R^2X 0.999 and Q^2 0.989 (Fig. 6A). The pairwise comparative OPLS-DA of IT-MS/MS data between α and β isomers presented significant intergroup discrepancy with good model quality of R^2X 0.861 and Q^2 0.988 (Fig. 6B). The parameters for the classification between Glc-Glc and Glc-Fru isomers were R^2X 0.999 and Q^2 0.994, suggesting that a good resolution could be achieved between isomers with different mono units (Fig. 6C). For the data sets generated from Q-TOF-MS/MS, disaccharide isomers could also be differentiated by OPLS-DA with good quality (Fig. 6D and Fig. S4). These results clearly demonstrated that disaccharide isomers could be rapidly discriminated through non-covalent leucine interactions by tandem mass spectrometry in combination with multivariate analysis.

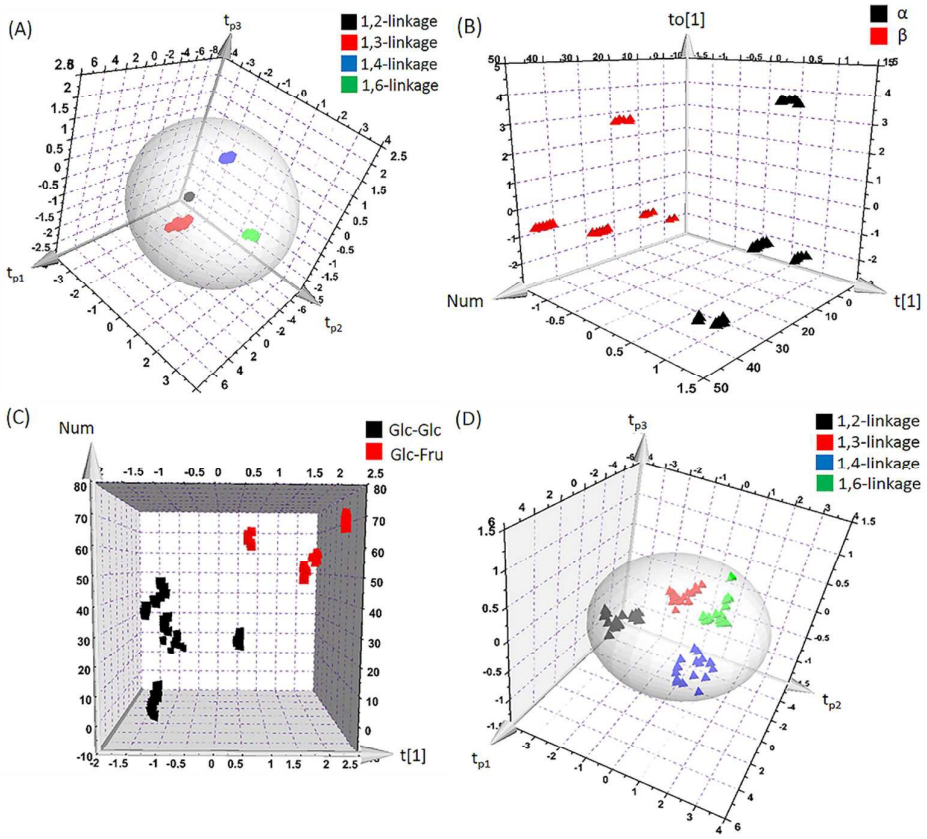

Fig.6 OPLS-DA differentiation of twelve glucose-containing disaccharidesbased on the fragmentation of ternary $[2Dis+Leu+K]^+$ complexes. (A) Discrimination of disaccharides with four position linkages by ESI-IT-MS/MS; (B) Discrimination of α isomers from β isomers by ESI-IT-MS/MS; (C) Discrimination of Glc-Glc from Glc-Fru by ESI-IT-MS/MS; (D) Discrimination of disaccharides with four position linkages by ESI-Q-TOF-MS/MS.

4. Conclusions

In summary, ESI-MS was firstly introduced to investigate the ternary complex of amino acids and disaccharides coordinated with H^+, NH_4^+, Li^+, Na^+, and K^+, respectively. The results showed that the formations of the ternary complexes were significantly influenced by the side chains of amino acids and cations attached. Notably, leucine could specifically interact with cellobiose to form stable complexes of $[Cello+Leu+K]^+$, $[Cello+2Leu+K]^+$, and $[2Cello+Leu+K]^+$ in gas phase using ESI-MS and the amount of their sugar-ring cleavage were dependent on the ratios of Cello-to-Leu. Among them, $[2Cello+Leu+K]^+$ could provide the most abundant fragmentation patterns and structural information. In combination of tandem mass spectrometry and stable isotope ^{18}O labeling technique, the structural conformation and fragmentation pathways of $[2Cello+Leu+K]^+$ were systematically investigated. It was found that the binding of leucine significantly induced the reducing ring opening rather than dissociation of non-covalent interactions, indicating that leucine might stabilize the non-covalent binding of the ternary complex and ultimately lead to fragment in a different pathway with the characteristic ions. Furthermore, this specific model was also applicable for other isomeric disaccharides. Based on this novel and general interactions of leucine with disaccharides, the discriminations among twelve disaccharide isomers with different linkages, mono units and anomeric configurations were successfully achieved by ESI-MS/MS in combination with PCA and OPLS-DA. The strategy demonstrated here will not only afford a rapid and easy method for disaccharide isomers differentiation using ESI-MS/MS, but also extend our understanding of the non-covalent interactions of amino acid, saccharides, and cations, which may offer the fresh perspective to investigate carbohydrate-protein interactions.

Acknowledgements

This work was supported by the Chinese National Natural Science Foundation (21232005, 21375113 and 21305115), the Natural Science Foundation of Fujian Province of China (2015J05035), the National Basic Research Program of China (2013CB910700) and the Fundamental Research Funds for the Central Universities (No. 20720150049).

Notes and references

1 A. Cerutti, M. Cols and I. Puga, *Nat. Rev. Immunol.,* 2013, **13**, 118-132.
2 R. Wang and D. R. Green, *Nat. Immunol.,* 2012, **13**, 907-915.
3 D. P. Gamblin, E. M. Scanlan, B. G. Davis, *Chem. Rev.*, 2009, **109**, 131-163.
4 Lis, N. Sharon, *Chem.Rev.,*1998, **98**, 637-674.
5 X. Li, Y. Pei, R. Zhang, Q. Shuai, F. Wang, T. Aastrup and Z. Pei, *Chem. Commun.,*2013, **49**, 9908-9910.
6 R. T. Sheridan, J. Hudon, J. A. Hank, P. M. Sondel and L. L. Kiessling, *ChemBioChem,*2014, **15**, 1393-1398.
7 C.Y. Huang, D. A. Thayer, A. Y. Chang, M. D. Best, J. Hoffmann, S. Head and C.H. Wong, *Proc. Natl. Acad. Sci. U. S. A.,*2006, **103**, 15-20.
8 X. Bi, D. Li and Z. Liu, *Anal. Chem.,* 2015, **87**, 4442-4447.
9 X. Sun and T. D. James, *Chem. Rev.,* 2015,**DOI:** 10.1021/cr500562m
10 Z. Xu, K. M. A. Uddin, T. Kamra, J. Schnadt and L. Ye, *ACS Appl. Mater. Inter.,* 2014, **6**, 1406-1414.
11 P. Shen and Y. Xia, *Anal. Chem.,* 2014, **86**, 5323-5329.
12 J. C. Munoz-Garcia, E. Chabrol, R. R. Vives, A. Thomas, J. L. De Paz, J. Rojo, A. Imberty, F. Fieschi, P. M. Nieto and J. Angulo, *J. Am. Chem. Soc.,*2015, **137**, 4100-4110.
13 L. P. Calle, B. Echeverria, A. Franconetti, S. Serna, M. C. Fernandez‐Alonso, T. Diercks, F. J. Cañada, A. Arda, N. C. Reichardt, and J. Jimenez‐Barbero, *Chem.- Eur. J.,*2015, **21**, 11408-11416.
14 A. Arda, P. Blasco, D. Varon Silva, V. Schubert, S. Andre, M. Bruix, F. J. Cañada, H.J. Gabius, C. Unverzagt and J. S. Jimenez-Barbero, *J. Am. Chem. Soc.,*2013, **135**, 2667-2675.
15 C. Laguri, N. Sapay, J.P. Simorre, B. Brutscher, A. Imberty, P. Gans and H. Lortat-Jacob, *J. Am. Chem. Soc.,*2011, **133**, 9642-9645.
16 S. Reichelt, C. Elsner, A. Prager, S. Naumov, J. Kuballa and M. R. Buchmeiser, *Analyst,*2012, **137**, 2600-2607.
17 M. C. Cook, S. J. Kaldas, G. Muradia, M. Rosu-Myles, J. P. Kunkel, *J. Chromatogr. B,*2015, **997**, 162-178.
18 W. R. Alley Jr, B. F. Mann, V. Hruska, M. V. Novotny, *Anal. Chem.,*2013, **85**, 10408-10416.
19 F. O. Gbormittah, B. B. Haab, K. Partyka, C. Garcia-Ott, M. Hancapie and W. S. Hancock, *J.Proteome Res.,*2013, **13**, 289-299.
20 S. E. Stefan, M. Ehsan, W. L. Pearson, A. Aksenov, V. Boginski, B. Bendiak and J. R. Eyler, *Anal. Chem.,* 2011, **83**, 8468-8476.
21 H. Gao, C. Petzold, M. Leavell and J. Leary, *J. Am. Soc. Mass Spectrom.,* 2003, **14**, 916-924.
22 W. Gabryelski and K. L. Froese, *J. Am. Soc. Mass Spectrom.,* 2003, **14**, 265-277.
23 N. C. Polfer, J. J. Valle, D. T. Moore, J. Oomens, J. R. Eyler and B. Bendiak, *Anal. Chem.,* 2006, **78**, 670-679.
24 Y. Tan and N. C. Polfer, *J. Am. Soc. Mass Spectrom.,* 2015, **26**, 359-368.
25 D. V. Augusti, F. Carazza, R. Augusti, W. A. Tao and R. G. Cooks, *Anal. Chem.,* 2002, **74**, 3458-3462.
26 C. Zu, B. N. Brewer, B. Wang, M. E. Koscho, *Anal. Chem.,* 2005, **77**, 5019-5027.
27 A. Mie, M. Jornten-Karlsson, B. O. Axelsson, A. Ray and C. T. Reimann, *Anal. Chem.,* 2007, **79**, 2850-2858.
28 C. S. R. Azenha, M. A. Coimbra, A. S. P. Moreira, P. Domingues and M. R. M. Domingues, *J. Mass Spectrom.,* 2013, **48**, 548-552.
29 A. Kuki, K. E. Szabo, L. Nagy, M. Zsuga and S. Keki, *J. Mass Spectrom.,* 2013, **48**, 1276-1280.
30 D. Wan, H. Yang, C. Yan, F. Song, Z. Liu and S. Liu, *Talanta,* 2013, **115**, 870-875.
31 B. Quemener, J. Vigouroux, E. Rathahao, J. C. Tabet, A. Dimitrijevic and M. Lahaye, *J. Mass Spectrom.,* 2015, **50**, 247-264.
32 Y. Cai and R. B. Cole, *Anal. Chem.* 2002, **74**, 985-991.
33 G. Li, Z. Huang, C. Fu, P. Xu, Y. Liu and Y. F. Zhao, *J. Mass Spectrom.,* 2010, **45**, 643-650.
34 E. V. da Costa, A. S. P. Moreira, F. M. Nunes, M. A. Coimbra and D. V. Evtuguin, M. R. M. Domingues, *Rapid Commun. Mass Spectrom.,* 2012, **26**, 2897-2904.
35 S. Cubbon, C. Antonio, J. Wilson and J. Thomas-Oates, *Mass Spectrum. Rev.,* 2010, **29**, 671-684.
36 M. Montowska, W. Rao, M. R. Alexander, G. A. Tucker and D. A. Barrett, *Anal. Chem.,* 2014, **86**, 4479-4487.
37 H. Wang, G. Yan, A. Zhang, Y. Li, Y. Wang, H. Sun, X. Wu and X. Wang, *Analyst,* 2013, **138**, 3303-3312.
38 H. Yuan, Y. L. Wu, W. Liu, Y. Liu, X. Gao, J. M. Lin and Y. F. Zhao, *Carbohydr. Res.,* 2015, **407**, 5-9.
39 H. J. An and C. B. Lebrilla, *Mass spectrometry reviews*, 2011, **30**, 560-578.
40 E. Lattova, S. Snovida, H. Perreault and O. Krokhin, *J. Am. Soc. Mass Spectrom.,* 2005, **16**, 683-696.
41 Y. Mechref, M. V. Novotny and C. Krishnan, *Anal. Chem.,* 2003, **75**, 4895-4903.
42 H. R. Yu, J. Q. Hu, X. H. Lu, X. J. Ju, Z. Liu, R. Xie, W. Wang and L. Y. Chu, *J. Phys. Chem. B.,* 2015, **119**, 1696-1705.
43 H. Sun, B. Ni, A. H. Zhang, M. Wang, H. Dong and X. J. Wang, *Analyst,* 2012, **137**, 170-185.
44 T. Zhang and D. G. Watson, *Analyst,* 2015, **140**, 2907-2915.
45 M. Li, B. Wang, M. Zhang, M. Rantalainen, S. Wang, H. Zhou, Y. Zhang, J. Shen, X. Pang, M. Zhang, H. Wei, Y. Chen, H. Lu, J. Zuo, M. Su, Y. Qiu, W. Jia, C. Xiao, L. M. Smith, S. Yang, E. Holmes, H. Tang, G. Zhao, J. K. Nicholson, L. Li and L. Zhao, *Proc. Natl. Acad. Sci. U. S. A.*, 2008, **105**, 2117-2122.
46 Y. Chen, J. Xu, R. Zhang, G. Shen, Y. Song, J. Sun, J. He, Q. Zhan and Z. Abliz, *Analyst,* 2013, **138**, 2669-2677.